Three-Dimensional Vibration Analysis of Toroidal Sectors With Solid Circular Cross-Sections

D. Zhou
Professor
College of Civil Engineering,
Nanjing University of Technology,
Xinmofan Road,
Nanjing 210009, People's Republic of China

Y. K. Cheung
Professor

S. H. Lo
Professor

Department of Civil Engineering,
University of Hong Kong,
Porkfulam Road,
Hong Kong, People's Republic of China

This paper studies the free vibration of circular toroidal sectors with circular cross-sections based on the three-dimensional small-strain, linear elasticity theory. A set of orthogonal coordinates, composing the polar coordinate (r, θ) with the origin on the cross-sectional centerline of the sector and the circumferential coordinate φ with the origin at the curvature center of the centerline, is developed to describe the displacements, strains, and stresses in the sector. Each of the displacement components is taken as a product of four functions: a set of Chebyshev polynomials in φ and r coordinates, a set of trigonometric series in θ coordinate, and a boundary function in terms of φ. Frequency parameters and mode shapes have been obtained via a displacement-based extremum energy principle. The upper bound convergence of the first eight frequency parameters accurate up to five figures has been achieved. The present results agree with those from the finite element solutions. The effect of the ratio of curvature radius R to the cross-sectional radius a and the subtended angle φ_0 on the frequency parameters of the sectors are discussed in detail. The three-dimensional vibration mode shapes are also plotted. [DOI: 10.1115/1.4000906]

Keywords: three-dimensional vibration, elasticity solution, toroidal sector, Ritz method, Chebyshev polynomial

1 Introduction

The plane toroidal sectors, also called as curved beams, partial rings, or arcs, are the common structural elements used in various engineering applications. The study on free vibration characteristics of toroidal sectors have been a subject of interest for many researchers and can be traced back to the 19th century [1,2]. While the dynamics of straight columns is well established and can be solved by fairly simple methods, the same cannot be said about toroidal sectors. The initial curvature of the toroidal sectors has been a source of difficulty and complexity in developing the governing relations between stress resultants and deformations, which include extension, flexure, shear and twist, etc.

A close scrutiny of the references reveals that to date, most of investigations on toroidal sector vibrations were carried out based on one-dimensional approximate theories [3]. In the one-dimensional models, the vibrations of a plane toroidal sector are commonly classified into the in-plane and out-of-plane ones and solved individually, if the principal plane of the cross-section contains the cross-sectional centerline of the undeformed sector and also a plane of material symmetry. Various one-dimensional models have been developed to analyze vibrations of toroidal sectors [4–7]. Archer [8] studied the in-plane inextensional vibrations of a toroidal sector based on the classical theory. Veletsos and Austin [9] investigated the effect of the extensibility of the sector axis and found that in some cases, the extensional and flexural motions are strongly coupled. Moreover, Austin and Veletsos [10] analyzed the effect of the rotary inertia and shear deformation on vibration characteristics of toroidal sectors. It is well known that one-dimensional dynamic models have serious limitation in the accuracy and applicable scope due to the imposed hypotheses. In one-dimensional models, all the variables have to be defined at the cross-sectional centerline of the sectors. The displacement and stress distributions within the cross-section are subjectively deduced based on certain assumptions. A typical approximation in one-dimensional models is to neglect the radial expansion/compression and axial warping of the cross-section. The existing research work shows that for a toroidal sector, the error of the one-dimensional models increases with the decrease in the ratio of the centerline curvature radius to the cross-sectional radius. Particularly, the error could remarkably rise with the decrease in the subtended angle.

The exact elasticity theory does not rely on any hypotheses involving the kinematics of deformation. Using the three-dimensional elasticity theory, a complete vibration spectrum for toroidal sectors can be computed, which cannot otherwise be predicted by the approximate theories. Such an analysis not only provides realistic results but also allows overall physical insights. Using a series expansion method, Hutchinson [11,12] analytically derived the accurate solutions for free vibrations of free-free solid cylinders. Leissa and Zhang [13] used the simple polynomials as admissible functions to study the free vibration of cantilevered rectangular parallelepiped based on the Ritz method. Lim [14] investigated the effect of neglecting transverse normal stress in the vibration analysis for cantilevered rectangular parallelepiped. Hutchinson [15] and Leissa and So [16] compared their respective three-dimensional elasticity solutions with the one-dimensional approximate solutions. Liew and co-workers [17,18] used orthogonal polynomials as the admissible functions to study free vibrations of elliptic sectors and prismatic columns with open sections of L, I, C, and I shapes. Recently, Zhou and co-workers [19,20] used the Chebyshev polynomials as admissible functions to study the vibrations of a solid and hollow circular cylinders and a torus with circular cross-section. Kang and Leissa [21,22] analyzed the vibration frequencies of closed rings with noncircular cross-sections. Buchanan and Liu [23] used the finite element method to analyze the free vibration of solid and hollow rings with circular cross-sections.

In this paper, the Ritz method is used to study the three-dimensional free vibration of circular toroidal sectors with circular cross-section. A set of orthogonal coordinates, a combination of

Contributed by the Applied Mechanics Division of ASME for publication in the JOURNAL OF APPLIED MECHANICS. Manuscript received September 16, 2008; final manuscript received December 10, 2009; published online March 31, 2010. Assoc. Editor: Wei-Chau Xie.

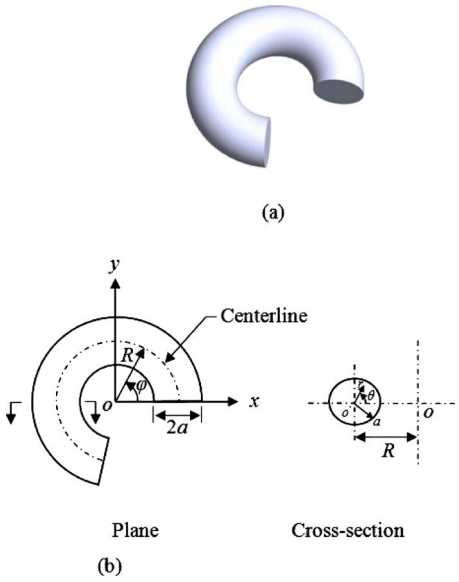

Fig. 1 A circular toroidal sector with circular cross-section. (*a*) 3D view and (*b*) coordinate system.

the polar coordinate (r,θ) on the center of each cross-section and the circumferential coordinate φ around the centerline of the sector are developed to describe the displacements, strains and stresses. The displacement components are taken to be u, v, and w in r, θ, and φ coordinates. The corresponding stress and strain components are ε_r, ε_θ, ε_φ, and $\gamma_{r\theta}$, $\gamma_{r\varphi}$, and $\gamma_{\theta\varphi}$. Each displacement component is expressed as a product of three separable series and a boundary function: a set Chebyshev polynomial series in the r and φ coordinates, a set of trigonometric series in the θ coordinate, and a geometric boundary function in terms of the φ coordinate. The eigenfrequencies and mode shapes are numerically calculated through the energy optimization process.

2 Formulation

Consider a circular toroidal sector with the circular cross-section as shown in Fig. 1. The cross-sectional radius of the sector is a. The subtended angle of the sector and the curvature radius of cross-sectional centerline are φ_0 and R $(R>a)$. A combination of the polar coordinate (r,θ) on the center of the cross-section and the circumferential coordinate φ along the cross-sectional centerline of the sector is chosen to describe the displacements, strains, and stresses. The polar coordinate (r,θ) describes the variables within the cross-section and the circumferential coordinate φ describes those along the direction normal to the cross-section. It is obvious that the three-dimensional coordinates (r,θ,φ) in this set are orthogonal to each other. The transformation relations between the Cartesian coordinates and the curved coordinates are given as follows:

$$x=(R+r\cos\theta)\cos\varphi;\quad y=(R+r\cos\theta)\sin\varphi;\quad z=r\sin\theta \tag{1}$$

From the above equation, the determinant of the Jacobian matrix of the coordinate system is given by

$$|J|=r(R+r\cos\theta) \tag{2}$$

Let u, v, and w, respectively, be the displacements in the r, θ, and φ directions, the relations between three-dimensional tensor strains and displacement components in the present coordinate system are given by

$$\varepsilon_r=\frac{\partial u}{\partial r},\quad \varepsilon_\theta=\frac{1}{r}\frac{\partial v}{\partial\theta}+\frac{u}{r}$$

$$\varepsilon_\varphi=\frac{1}{R+r\cos\theta}\frac{\partial w}{\partial\varphi}+\frac{\cos\theta}{R+r\cos\theta}u-\frac{\sin\theta}{R+r\cos\theta}v$$

$$\gamma_{r\theta}=\frac{\partial v}{\partial r}-\frac{v}{r}+\frac{1}{r}\frac{\partial u}{\partial\theta},\quad \gamma_{\theta\varphi}=\frac{1}{r}\frac{\partial w}{\partial\theta}+\frac{\sin\theta}{R+r\cos\theta}w+\frac{1}{R+r\cos\theta}\frac{\partial v}{\partial\varphi} \tag{3}$$

$$\gamma_{\varphi r}=\frac{1}{R+r\cos\theta}\frac{\partial u}{\partial\varphi}+\frac{\partial w}{\partial r}-\frac{\cos\theta}{R+r\cos\theta}w$$

Therefore, the strain energy V and the kinetic energy T of the sector undergoing free vibration are

$$V=(1/2)\int_0^{\varphi_0}\int_0^{2\pi}\int_0^{a}[(\lambda+2G)\varepsilon_r^2+2\lambda\varepsilon_r\varepsilon_\theta+2\lambda\varepsilon_r\varepsilon_\varphi+(\lambda+2G)\varepsilon_\theta^2+2\lambda\varepsilon_\theta\varepsilon_\varphi+(\lambda+2G)\varepsilon_\varphi^2+G(\gamma_{r\theta}^2+\gamma_{\theta\varphi}^2+\gamma_{\varphi r}^2)]\times|J|drd\theta d\varphi,$$

$$T=(\rho/2)\int_0^{\varphi_0}\int_0^{2\pi}\int_0^{a}(\dot u^2+\dot v^2+\dot w^2)|J|drd\theta d\varphi \tag{4}$$

where ρ is the constant mass per unit volume, $\dot u$, $\dot v$, and $\dot w$ are the velocity components. The parameters λ and G are the Lamé constants for a homogeneous and isotropic material, which are expressed in terms of Young's modulus E and Poisson's ratio ν by

$$\lambda=\nu E/[(1+\nu)(1-2\nu)];\quad G=E/[2(1+\nu)] \tag{5}$$

Defining the following dimensionless coordinates

$$\bar R=R/a,\quad \bar r=r/a,\quad \bar\varphi=\varphi/\varphi_0 \tag{6}$$

In the free vibrations, the displacement components may be expressed as

$$u=U(\bar r,\theta,\bar\varphi)e^{i\omega t},\quad v=V(\bar r,\theta,\bar\varphi)e^{i\omega t},\quad w=W(\bar r,\theta,\bar\varphi)e^{i\omega t} \tag{7}$$

where ω is the circular eigenfrequency of the sector and $i=\sqrt{-1}$.

Substituting Eqs. (6) and (7) into Eq. (4) gives the maximums of strain and kinetic energies.

$$V_{\max}=(Ga\varphi_0/2)\int_0^1\int_0^{2\pi}\int_0^1[(\bar\lambda+2)\bar\varepsilon_r^2+2\bar\lambda\bar\varepsilon_r\bar\varepsilon_\theta+2\bar\lambda\bar\varepsilon_r\bar\varepsilon_\varphi+(\bar\lambda+2)\bar\varepsilon_\theta^2+2\bar\lambda\bar\varepsilon_\theta\bar\varepsilon_\varphi+(\bar\lambda+2)\bar\varepsilon_\varphi^2+\bar\gamma_{r\theta}^2+\bar\gamma_{\theta\varphi}^2+\bar\gamma_{\varphi r}^2]\times(\bar R+\bar r\cos\theta)\bar r d\bar r d\theta d\bar\varphi,$$

$$T_{\max}=(\rho a^3\varphi_0\omega^2/2)\int_0^1\int_0^{2\pi}\int_0^1(U^2+V^2+W^2)\times(\bar R+\bar r\cos\theta)\bar r d\bar r d\theta d\bar\varphi \tag{8}$$

in which

$$\bar\lambda=\frac{2\nu}{1-2\nu},\quad \bar\varepsilon_r^2=\left(\frac{\partial U}{\partial\bar r}\right)^2,\quad \bar\varepsilon_\theta^2=\frac{1}{\bar r^2}\left[\left(\frac{\partial V}{\partial\theta}\right)^2+2U\frac{\partial V}{\partial\theta}+U^2\right]$$

$$\bar\varepsilon_\varphi^2=\frac{1}{(\bar R+\bar r\cos\theta)^2}\left[\frac{1}{\varphi_0^2}\left(\frac{\partial W}{\partial\bar\varphi}\right)^2+\frac{2\cos\theta}{\varphi_0}U\frac{\partial W}{\partial\bar\varphi}-\frac{2\sin\theta}{\varphi_0}V\frac{\partial W}{\partial\bar\varphi}+\cos^2\theta U^2-\sin(2\theta)UV+\sin^2\theta V^2\right]$$

$$\bar\varepsilon_r\bar\varepsilon_\theta=\frac{1}{\bar r}\left(\frac{\partial U}{\partial\bar r}\frac{\partial V}{\partial\theta}+U\frac{\partial U}{\partial\bar r}\right)$$

$$\bar{\varepsilon}_\theta \bar{\varepsilon}_\varphi = \frac{1}{\bar{r}(\bar{R}+\bar{r}\cos\theta)}\left[\frac{1}{\varphi_0}\left(\frac{\partial V}{\partial\theta}\frac{\partial W}{\partial\bar{\varphi}}+U\frac{\partial W}{\partial\bar{\varphi}}\right)+\cos\theta\left(U\frac{\partial V}{\partial\theta}+U^2\right)-\sin\theta\left(V\frac{\partial V}{\partial\theta}+UV\right)\right]$$

$$\bar{\varepsilon}_\varphi \bar{\varepsilon}_r = \frac{1}{\bar{R}+\bar{r}\cos\theta}\left[\frac{1}{\varphi_0}\frac{\partial U}{\partial\bar{r}}\frac{\partial W}{\partial\bar{\varphi}}+\cos\theta U\frac{\partial U}{\partial\bar{r}}-\sin\theta\frac{\partial U}{\partial\bar{r}}V\right] \tag{9}$$

$$\bar{\gamma}_{r\theta}^2 = \left(\frac{\partial V}{\partial\bar{r}}\right)^2-\frac{2}{\bar{r}}V\frac{\partial V}{\partial\bar{r}}+\frac{2}{\bar{r}}\frac{\partial U}{\partial\theta}\frac{\partial V}{\partial\bar{r}}+\frac{1}{\bar{r}^2}V^2-\frac{2}{\bar{r}^2}\frac{\partial U}{\partial\theta}V+\frac{1}{\bar{r}^2}\left(\frac{\partial U}{\partial\theta}\right)^2$$

$$\bar{\gamma}_{\theta\varphi}^2 = \frac{1}{\bar{r}^2}\left(\frac{\partial W}{\partial\theta}\right)^2+\frac{2}{\bar{r}(\bar{R}+\bar{r}\cos\theta)}\left(\sin\theta W\frac{\partial W}{\partial\theta}+\frac{1}{\varphi_0}\frac{\partial V}{\partial\bar{\varphi}}\frac{\partial W}{\partial\theta}\right)+\frac{1}{(\bar{R}+\bar{r}\cos\theta)^2}\left[\sin^2\theta W^2+\frac{2\sin\theta}{\varphi_0}\frac{\partial V}{\partial\bar{\varphi}}W+\frac{1}{\varphi_0^2}\left(\frac{\partial V}{\partial\bar{\varphi}}\right)^2\right]$$

$$\bar{\gamma}_{\varphi r}^2 = \left(\frac{\partial W}{\partial\bar{r}}\right)^2+\frac{2}{\bar{R}+\bar{r}\cos\theta}\left(\frac{1}{\varphi_0}\frac{\partial U}{\partial\bar{\varphi}}\frac{\partial W}{\partial\bar{r}}-\cos\theta W\frac{\partial W}{\partial\bar{r}}\right)+\frac{1}{(\bar{R}+\bar{r}\cos\theta)^2}\left[\frac{1}{\varphi_0^2}\left(\frac{\partial U}{\partial\bar{\varphi}}\right)^2-\frac{2\cos\theta}{\varphi_0}\frac{\partial U}{\partial\bar{\varphi}}W+\cos^2\theta W^2\right]$$

The Lagrangian energy functional Π of the sector is given by

$$\prod = T_{\max} - V_{\max} \tag{10}$$

The displacement functions $U(\bar{r},\theta,\bar{\varphi})$, $V(\bar{r},\theta,\bar{\varphi})$, and $W(\bar{r},\theta,\bar{\varphi})$ are expressed in terms of finite series as

$$U(\bar{r},\theta,\bar{\varphi}) = D_u(\bar{\varphi})\sum_{i=1}^{I}\sum_{j=1}^{J}\sum_{k=1}^{K}A_{ijk}F_i(\bar{r})H_j(\theta)F_k(\bar{\varphi})$$

$$V(\bar{r},\theta,\bar{\varphi}) = D_v(\bar{\varphi})\sum_{l=1}^{L}\sum_{m=1}^{M}\sum_{n=1}^{N}B_{lmn}F_l(\bar{r})\bar{H}_m(\theta)F_k(\bar{\varphi}) \tag{11}$$

$$\bar{W}(\bar{r},\theta,\bar{\varphi}) = D_w(\bar{\varphi})\sum_{p=1}^{P}\sum_{q=1}^{Q}\sum_{s=1}^{S}C_{pqs}F_p(\bar{r})H_q(\theta)F_s(\bar{\varphi})$$

where $D_u(\bar{\varphi})$, $D_v(\bar{\varphi})$, and $D_w(\bar{\varphi})$ are the boundary functions, which describe the boundary conditions of the sector at two ends $\varphi=0$ and $\varphi=\varphi_0$. A_{ijk}, B_{lmn}, and C_{pqs} are the undetermined coefficients and I, J, K, L, M, N, P, Q, and S are the truncated orders of their corresponding series. $F_i(\bar{r})$, $F_j(\bar{r})$, $F_k(\bar{r})$, $F_p(\bar{\varphi})$, $F_q(\bar{\varphi})$, and $F_s(\bar{\varphi})$ are the Chebyshev polynomials of first kind, which can be systematically expressed as

$$F_i(\chi) = \cos[(i-1)\arccos(2\chi-1)], \quad i=1,2,3,\ldots, \quad \chi=\bar{r},\bar{\varphi} \tag{12}$$

It is noted that in using the Ritz method, the stress boundary conditions of the sectors need not be satisfied in advance but the geometric boundary conditions should be satisfied exactly. There is no displacement restraint on the curved surface of the sector. Therefore, the boundary functions $D_u(\bar{\varphi})$, $D_v(\bar{\varphi})$, and $D_w(\bar{\varphi})$ are sufficient to enable the displacement components u, v, and w satisfying the geometric boundary conditions at the two ends of the sector, which are listed in Table 1. It should be mentioned that the Chebyshev polynomials has two distinct advantages. One is that $F_i(\chi)$ $(i=1,2,3,\ldots)$ is a set of complete and orthogonal series in the interval $[-1,1]$, which is more stable in numerical computations than other admissible functions such as the simple algebraic polynomials. The other advantage is that $F_i(\chi)$ $(i=1,2,3,\ldots)$ can be expressed in a simple and unified form of cosine functions,

Table 1 The boundary functions for common end conditions

End conditions	$D_u(\bar{\varphi})$	$D_v(\bar{\varphi})$	$D_w(\bar{\varphi})$
Clamped-clamped	$\bar{\varphi}(1-\bar{\varphi})$	$\bar{\varphi}(1-\bar{\varphi})$	$\bar{\varphi}(1-\bar{\varphi})$
Clamped-free	$\bar{\varphi}$	$\bar{\varphi}$	$\bar{\varphi}$
Clamped-sliding	$\bar{\varphi}$	$\bar{\varphi}$	$\bar{\varphi}(1-\bar{\varphi})$
Clamped-hard pinned	$\bar{\varphi}(1-\bar{\varphi})$	$\bar{\varphi}(1-\bar{\varphi})$	$\bar{\varphi}$
Clamped-soft pinned	$\bar{\varphi}(1-\bar{\varphi})$	$\bar{\varphi}$	$\bar{\varphi}$
Free-free	1	1	1
Hard pinned-hard pinned	$\bar{\varphi}(1-\bar{\varphi})$	$\bar{\varphi}(1-\bar{\varphi})$	1
Hard pinned-soft pinned	$\bar{\varphi}(1-\bar{\varphi})$	$\bar{\varphi}$	1
Sliding-sliding	1	1	$\bar{\varphi}(1-\bar{\varphi})$
Soft pinned-soft pinned	$\bar{\varphi}(1-\bar{\varphi})$	1	1

Note: "Hard pinned" means the zero displacement restraints both for u and for v at the end. "Soft pinned" means the zero displacement restraint only for u at the end.

which is easier for coding than the orthogonal recurrent polynomials constructed from the Schmidt process. It is obvious that the completeness and orthogonality of the admissible functions in the $\bar{\varphi}$ direction are destroyed by the boundary functions, except for the free-free ends. However, the boundary functions used here are positive in the interval (0,1). It means the boundary functions are ineffective to the zero point distribution of the admissible functions within the domain. They can only adjust the value distribution of the admissible functions. Therefore, the main properties of the Chebyshev polynomials are still reserved. We can conclude that there is no frequency lost in the present analysis if enough terms of admissible functions are used.

It is obvious that a plane toroidal sector with circular cross-section is symmetric about its centerline plane (i.e., a plane containing the centerline of the sector). Therefore, the vibrations of the sectors made of isotropic material can be classified into two distinct categories: symmetric and antisymmetric vibrations about the centerline plane. For the symmetric vibration about the centerline plane, one has

$$H_s(\theta) = \cos[(s-1)\theta], \quad \bar{H}_s(\theta) = \sin(s\theta), \quad s=1,2,3,\ldots \tag{13}$$

and for the antisymmetric vibration about the centerline plane, one has

$$H_s(\theta) = \sin(s\theta), \quad \bar{H}_s(\theta) = \cos[(s-1)\theta], \quad s=1,2,3,\ldots \tag{14}$$

Each of these two categories can be separately solved and thus it results in a smaller set of eigenvalue equations while maintaining the same level of accuracy.

Minimizing functional (10) with respect to the coefficients of displacement functions, i.e.,

$$\frac{\partial\Pi}{\partial A_{ijk}}=0, \quad \frac{\partial\Pi}{\partial B_{lmn}}=0, \quad \frac{\partial\Pi}{\partial C_{pqs}}=0 \tag{15}$$

leads to the following eigenfrequency equation:

$$\left[\begin{pmatrix}[K_{uu}] & [K_{uv}] & [K_{uw}]\\ & [K_{vv}] & [K_{vw}]\\ \text{Sym} & & [K_{ww}]\end{pmatrix}-\Omega^2\begin{pmatrix}[M_{uu}] & [0] & [0]\\ & [M_{vv}] & [0]\\ \text{Sym} & & [M_{ww}]\end{pmatrix}\right]\begin{Bmatrix}\{A\}\\ \{B\}\\ \{C\}\end{Bmatrix}=\begin{Bmatrix}\{0\}\\ \{0\}\\ \{0\}\end{Bmatrix} \tag{16}$$

where $\Omega=\omega a\sqrt{\rho/G}$ and

Table 2 The Convergence of the first eight frequency parameters for a C-C circular toroidal sector with subtended angle $\varphi_0=90$ deg and radius ratio $R/a=2$

$I\times J\times K$	Ω_1	Ω_2	Ω_3	Ω_4	Ω_5	Ω_6	Ω_7	Ω_8
Symmetric vibrations about the centerline plane								
$6\times3\times12$	1.1245	1.2861	1.7230	2.3568	2.5627	2.5967	2.7290	2.9240
$8\times4\times16$	1.1236	1.2856	1.7222	2.3557	2.5592	2.5949	2.7208	2.9182
$10\times5\times20$	1.1235	1.2854	1.7221	2.3555	2.5588	2.5947	2.7204	2.9179
$12\times6\times24$	1.1234	1.2853	1.7220	2.3553	2.5587	2.5947	2.7203	2.9178
$14\times7\times28$	1.1234	1.2853	1.7220	2.3553	2.5587	2.5947	2.7203	2.9178
Antisymmetric vibrations about the centerline plane								
$6\times3\times12$	0.73384	1.3316	1.3427	2.1331	2.2778	2.4976	2.5421	2.8668
$8\times4\times16$	0.73321	1.3316	1.3423	2.1327	2.2773	2.4971	2.5395	2.8604
$10\times5\times20$	0.73305	1.3315	1.3422	2.1327	2.2773	2.4970	2.5392	2.8601
$12\times6\times24$	0.73299	1.3315	1.3422	2.1326	2.2772	2.4970	2.5391	2.8600
$14\times7\times28$	0.73299	1.3315	1.3422	2.1326	2.2772	2.4970	2.5391	2.8600

$$\{A\}=\begin{Bmatrix} A_{111}\\ A_{112}\\ \vdots\\ A_{11K}\\ A_{121}\\ \vdots\\ A_{12K}\\ \vdots\\ A_{1JK}\\ \vdots\\ A_{IJK}\end{Bmatrix},\quad \{B\}=\begin{Bmatrix} B_{111}\\ B_{112}\\ \vdots\\ B_{11N}\\ B_{121}\\ \vdots\\ B_{12N}\\ \vdots\\ B_{1MN}\\ \vdots\\ B_{LMN}\end{Bmatrix},\quad \{C\}=\begin{Bmatrix} C_{111}\\ C_{112}\\ \vdots\\ C_{11S}\\ C_{121}\\ \vdots\\ C_{12S}\\ \vdots\\ C_{1QS}\\ \vdots\\ C_{PQS}\end{Bmatrix} \tag{17}$$

Each element in matrices $[K_{ij}]$ and $[M_{ij}]$ $(i,j=u,v,w)$ can be numerically evaluated. By solving Eq. (16), the total $I\times J\times K+L\times M\times N+P\times Q\times R$ eigenvalues and corresponding modes can be obtained.

3 Convergence

To guarantee the accuracy of frequencies obtained by the procedure described above, it is necessary to conduct some convergence studies to determine the number of terms required in the series of Eq. (11). A convergence study is based upon the fact that all the frequencies obtained by the Ritz method should converge to their exact values in an upper bound manner. For simplicity, equal numbers of terms of admissible functions are taken in displacement amplitude functions U, V, and W although different numbers of terms among U, V, and W might provide a more rapid convergence. Tables 2 and 3 give the convergence studies of first seven frequency parameters $\Omega_i=\omega_i a\sqrt{\rho/G}$ $(i=1,2,\ldots,7)$ of a sector with two different end conditions: clamped two ends and free two ends, respectively. For the free-free sector, six zero-frequencies are excluded in the present analysis. The subtended angle of the sector is $\varphi_0=90$ deg and the radius ratio is $R/a=2$. In all of the following analyses, the Poisson's ratio is fixed at $\nu=0.3$. The eigenfrequencies of the symmetric and antisymmetric vibration modes about the centerline plane of the sector are separately given. The computations were performed in double precision (16 significant figures) and piecewise Gaussian quadrature was used numerically to evaluate the integrations when the eigenfrequency Eq. (16) was produced. It is shown from Tables 2 and 3 that the excellent convergence has been achieved. In general, $12\times6\times24$ terms can give the solutions with at least five significant figures. Moreover, one can find that the convergence of eigenfrequencies for the sector with F-F ends is somewhat more rapid than that for the sector with C-C ends. It is obvious that for a F-F sector, the admissible functions for every displacement components are a complete set in three directions where the boundary functions are equal to 1. However, for a C-C sector, the admissible functions are not a complete set in the φ direction due to the nonconstant boundary functions about φ.

4 Comparisons

In approximate one-dimensional theories, the vibrations of plane toroidal sectors were commonly divided into two categories for the analysis: in-plane vibrations and out-of-plane vibrations. In the present analysis, the symmetric vibrations about the centerline plane of the sector correspond to the in-plane vibrations of the

Table 3 The Convergence of the first eight nonzero frequency parameters for a F-F circular toroidal sector with subtended angle $\varphi_0=90$ deg and radius ratio $R/a=2$

$I\times J\times K$	Ω_1	Ω_2	Ω_3	Ω_4	Ω_5	Ω_6	Ω_7	Ω_8
Symmetric vibrations about the centerline plane								
$6\times3\times12$	1.0686	1.5280	1.7444	2.1364	2.2280	2.3360	2.3974	2.5423
$8\times4\times16$	1.0671	1.5278	1.7430	2.1293	2.2114	2.3338	2.3967	2.5413
$10\times5\times20$	1.0670	1.5278	1.7430	2.1292	2.2107	2.3337	2.3967	2.5413
$12\times6\times24$	1.0670	1.5278	1.7430	2.1292	2.2106	2.3337	2.3967	2.5413
$14\times7\times28$	1.0670	1.5278	1.7430	2.1292	2.2106	2.3337	2.3967	2.5413
Antisymmetric vibrations about the centerline plane								
$6\times3\times12$	1.0150	1.0642	1.6800	1.9781	2.1180	2.2787	2.2930	2.4379
$8\times4\times16$	1.0143	1.0640	1.6789	1.9740	2.1154	2.2744	2.2915	2.4273
$10\times5\times20$	1.0143	1.0640	1.6789	1.9738	2.1154	2.2743	2.2915	2.4270
$12\times6\times24$	1.0143	1.0640	1.6789	1.9738	2.1154	2.2743	2.2915	2.4270
$14\times7\times28$	1.0143	1.0640	1.6789	1.9738	2.1154	2.2743	2.2915	2.4270

Table 4 The comparison of the first four in-plane frequency parameters $\Omega_i(R/a)^2\sqrt{2/(1+\nu)}$ ($i=1,2,3,4$) of C-C circular toroidal sectors with circular cross-sections

		$\varphi_0=60$ deg		$\varphi_0=120$ deg		$\varphi_0=180$ deg	
R/a	i	Present	Ref. 7	Present	Ref. 7	Present	Ref. 7
10	1	24.08^s	23.75	10.76^a	10.61	4.202^a	4.151
	2	39.69^a	39.05	15.32^s	15.19	8.637^s	8.502
	3	63.06^a	62.38	25.00^s	24.72	15.63^a	15.46
	4	71.87^s	70.71	30.77^a	30.47	18.04^s	17.91
50	1	53.01^a	52.82	11.81^a	11.79	4.382^a	4.374
	2	76.13^s	76.01	23.30^s	23.25	9.619^s	9.603
	3	118.2^s	117.9	42.46^a	42.37	17.84^a	17.81
	4	171.7^a	171.1	61.55^s	61.43	27.26^s	27.22

Note: The superscript s means symmetric modes in the φ direction and the superscript a means antisymmetric modes in the φ direction.

one-dimensional theories while the antisymmetric vibrations about the centerline plane of the sector correspond to the out-of-plane vibrations of the one-dimensional theories. A comparison of the present results with those obtained from the one-dimensional Timoshenko theory [6,7] is given in Tables 4 and 5, respectively. The sectors are clamped at two ends. Two different radius ratios $R/a=10$ and $R/a=50$ and three different subtended angles $\varphi_0=60$ deg, $\varphi_0=120$ deg, and $\varphi_0=180$ deg are considered. For the consistency with the references, the frequency parameter $\omega R\sqrt{\rho A/(EI)}=\Omega(R/a)^2\sqrt{2/(1+\nu)}$ is used for comparison, where A and I are the area and inertia moment of the cross-section, respectively. It can be seen that the present results agree with the one-dimensional approximate solutions. The more the radius ratio R/a and the subtended angle φ_0, the closer are the two kinds of solutions.

5 Results

For thick curved sectors, the one-dimensional theories would bring considerable errors. In such a case, the three-dimensional elasticity analysis can provide more accurate results. Tables 6 and 7 give the first eight frequency parameters of symmetric and antisymmetric vibrations about the centerline plane for the sectors with free two ends, respectively. Five different radius ratios $R/a=1.5$, 2.0, 3.0 5.0, and 10.0 and three different subtended angles $\varphi_0=60$ deg, 120 deg, and 180 deg are examined. From these two tables, it is seen that the eigenfrequencies monotonically decrease with the increase in the radius ratio R/a and the subtended angle φ_0. When the sector makes symmetric vibration about its centerline plane, the lowest eigenfrequency belongs to the antisymmetric modes in the φ direction, except for the case of $R/a=1.5$ and $\varphi_0=60$ deg. Figure 2 gives the first frequencies of symmetric and antisymmetric modes about φ for circular toroidal sectors with clamped two ends when the sectors make symmetric vibrations about their centerline plane. Figure 3 gives those when the sectors make antisymmetric vibrations about their centerline plane. The frequency parameter $\Lambda=\omega R\sqrt{\rho A/(EI)}=\Omega(R/a)^2\sqrt{2/(1+\nu)}$ is used to show the variation in eigenfrequencies with respect to the radius ratio R/a within the interval [1.5,50]. One can see from Fig. 2 that when the sector makes symmetric vibrations about its centerline plane, the eigenfrequencies of the symmetric modes about φ are always higher than those of the antisymmetric modes about φ. However, one can see from Fig. 3 that when the sector makes antisymmetric vibrations about its centerline plane, the eigenfrequencies of the symmetric modes about φ are always lower than those of the antisymmetric modes about φ. It is seen from these two figures that with the increase in the radius ratio, all frequency parameters monotonically approach to their respective constants. The bigger the subtended angle, the quicker is the rate close to the constants with the increase in the radius ratio. Moreover, it is seen that for thick sectors (smaller R/a, for example $R/a<5.0$), the frequency parameters rapidly vary, especially for the larger subtended angles. When the sector makes symmetric vibrations about its centerline plane, the frequency parameters of symmetric modes about φ vary more quickly than those of antisymmetric modes about φ. However, when the sector makes antisymmetric vibrations about its centerline plane, the frequency parameters of antisymmetric modes about φ vary more quickly than those of the symmetric modes about φ. It can be concluded from Figs. 2 and 3 that for thick curved beams, the one-dimensional theories cannot accurately predict the eigenfrequencies of the beams because the effect of the radius ratio R/a on the frequency parameter Λ is always quite small in the one-dimensional analysis. Finally, the first four three-dimensional mode shapes of a sector with radius ratio $R/a=2.0$ and subtended

Table 5 The comparison of the first four out-of-plane frequency parameters $\Omega_i(R/a)^2\sqrt{2/(1+\nu)}$ ($i=1,2,3,4$) of C-C circular toroidal sectors with circular cross-sections

		$\varphi_0=60$ deg		$\varphi_0=120$ deg		$\varphi_0=180$ deg	
R/a	i	Present	Ref. 6	Present	Ref. 6	Present	Ref. 6
10	1	16.96^s	16.88	4.322^s	4.309	1.795^s	1.791
	2	40.21^s	39.70	11.79^a	11.79	5.030^a	5.032
	3	41.00^a	40.90	22.54^s	22.50	10.21^s	10.23
	4	70.64^s	70.51	23.50^s	23.30	16.88^a	16.91
50	1	19.51^s	19.45	4.480^s	4.473	1.820^s	1.818
	2	54.30^a	54.14	12.91^a	12.89	5.247^a	5.242
	3	106.2^s	105.9	26.12^s	26.08	11.00^s	10.99
	4	173.7^a	173.1	43.75^a	43.68	18.83^a	18.81

Note: The superscript s means symmetric modes in the φ direction and the superscript a means antisymmetric modes in the φ direction.

Table 6 The first eight nonzero frequency parameters $\Omega_i=\omega_i a\sqrt{\rho/G}$ ($i=1,2,\ldots,8$) of F-F circular toroidal sectors with circular cross-sections for symmetric vibrations about the centerline plane of sectors

R/a	Ω_1	Ω_2	Ω_3	Ω_4	Ω_5	Ω_6	Ω_7	Ω_8
				$\varphi_0=60$ deg				
1.5	1.9369^a	1.9790^s	2.4254^s	2.5214^a	2.5725^s	2.7478^s	2.7940^a	3.0174^s
2.0	1.6743^s	2.0222^a	2.1152^s	2.1925^a	2.4030^s	2.5841^s	2.8119^s	2.8265^a
3.0	1.0864^s	1.5448^s	1.7432^a	2.1149^a	2.1810^s	2.3373^s	2.4480^a	2.5832^s
5.0	0.4987^s	0.9800^s	1.0435^a	1.6151^s	1.7979^s	1.9154^a	2.1300^s	2.1361^a
10.0	0.1466^s	0.3640^a	0.5045^s	0.6320^s	0.9167^a	0.9658^a	1.2116^s	1.4151^s
				$\varphi_0=120$ deg				
1.5	1.0398^s	1.5217^s	1.7183^a	2.1421^a	2.2300^s	2.3357^s	2.3446^a	2.5339^a
2.0	1.2369^s	1.3425^a	1.9324^a	1.9544^s	2.1875^a	2.2021^a	2.2240^a	2.4322^a
3.0	0.3485^s	0.7925^a	0.8932^s	1.2959^s	1.4863^a	1.7121^a	2.0325^s	2.0849^a
5.0	0.1365^s	0.3495^a	0.5617^s	0.6241^s	0.9045^a	0.9824^a	1.2035^s	1.4000^s
10.0	0.0357^s	0.0993^a	0.1911^s	0.2887^s	0.3024^a	0.4276^s	0.5045^a	0.5624^a
				$\varphi_0=180$ deg				
1.5	0.5449^s	1.1355^a	1.2167^s	1.6965^a	1.7290^s	2.0786^a	2.1733^s	2.2682^a
2.0	0.3284^s	0.7614^a	0.9865^s	1.2909^s	1.4332^a	1.6964^a	1.9158^s	2.0606^s
3.0	0.1547^s	0.3931^a	0.6801^s	0.7499^s	1.0175^a	1.1108^a	1.3566^s	1.5020^s
5.0	0.0578^s	0.1576^a	0.3047^s	0.4479^s	0.4779^a	0.6661^s	0.6965^a	0.8621^a
10.0	0.0147^s	0.0418^a	0.0854^s	0.1416^a	0.2078^s	0.2270^s	0.2823^a	0.3576^a

Note: The superscript s means symmetric modes in the φ direction and the superscript a means antisymmetric modes in the φ direction.

angle $\varphi_0=180$ deg are given in Figs. 4 and 5 for the symmetric and antisymmetric vibrations about its centerline plane. The corresponding frequency parameters are also given under the figures.

6 Conclusions

Based on the exact, small-strain and linear elasticity theory, the three-dimensional free vibration characteristics of plane circular toroidal sectors with circular cross-section have been studied. The spatial integrals for strain and kinetic energies have been formulated by developing a set of orthogonal coordinates. By means of the Ritz method, the governing eigenfrequency equations are derived through the minimization of the extremum of energy functional. A combination of the Chebyshev polynomial series, the trigonometric series and a boundary function are taken as admissible functions of each displacement component. By using the structural symmetry about the centerline plane, the vibrations of a sector are classified into two distinct categories, namely, the symmetric and antisymmetric vibration modes about its centerline plane, which can be computed and studied separately. The convergence of first eight eigenfrequencies has been examined and accurate results at least with five significant figures have been achieved. The present analysis provides the complete vibration

Table 7 The first eight nonzero frequency parameters $\Omega_i=\omega_i a\sqrt{\rho/G}$ ($i=1,2,\ldots,8$) of F-F circular toroidal sectors with circular cross-sections for antisymmetric vibrations about the centerline plane of sectors

R/a	Ω_1	Ω_2	Ω_3	Ω_4	Ω_5	Ω_6	Ω_7	Ω_8
				$\varphi_0=60$ deg				
1.5	1.7987^s	2.0030^a	2.0895^s	2.4916^a	2.5160^s	2.8456^a	3.0237^a	3.0834^s
2.0	1.5481^s	1.6374^a	2.0364^s	2.1412^s	2.3893^a	2.4715^a	2.8393^a	2.9998^s
3.0	1.0332^s	1.0516^a	1.7007^s	2.0166^a	2.1113^s	2.2350^a	2.3410^a	2.3683^s
5.0	0.5125^a	0.6012^s	1.0312^s	1.2266^a	1.5831^a	1.7791^s	1.9533^s	2.1283^a
10.0	0.1719^a	0.2832^s	0.3838^s	0.5846^a	0.6513^a	0.8807^s	0.9414^s	1.1751^a
				$\varphi_0=120$ deg				
1.5	0.9903^s	1.0843^a	1.6678^a	1.9122^s	2.1261^a	2.2480^a	2.2525^s	2.5031^s
2.0	0.7088^s	0.7806^a	1.2805^a	1.5865^s	1.9166^s	1.9383^a	2.1206^a	2.1936^s
3.0	0.4229^s	0.4799^a	0.8011^a	1.0394^s	1.2607^s	1.5008^a	1.7346^a	1.8867^s
5.0	0.2187^s	0.2506^s	0.4100^a	0.5600^s	0.6800^s	0.8493^a	0.9759^a	1.1370^s
10.0	0.0829^a	0.0944^s	0.1763^a	0.1907^s	0.3010^a	0.3158^s	0.4244^s	0.4631^a
				$\varphi_0=180$ deg				
1.5	0.6553^s	0.6606^a	1.1282^a	1.3811^s	1.7437^s	1.7683^a	2.0772^a	2.1354^s
2.0	0.4474^a	0.4744^s	0.8078^a	1.0296^s	1.2967^s	1.4408^a	1.7862^a	1.8030^s
3.0	0.2518^a	0.3006^s	0.4945^a	0.6230^s	0.8095^s	0.9293^a	1.1508^a	1.2337^s
5.0	0.1122^a	0.1674^s	0.2679^a	0.3015^s	0.4621^a	0.4532^s	0.6398^s	0.6505^a
10.0	0.0319^a	0.0642^s	0.1118^s	0.1123^a	0.1596^a	0.1956^s	0.2337^s	0.2748^a

Note: The superscript s means symmetric modes in the φ direction and the superscript a means antisymmetric modes in the φ direction.

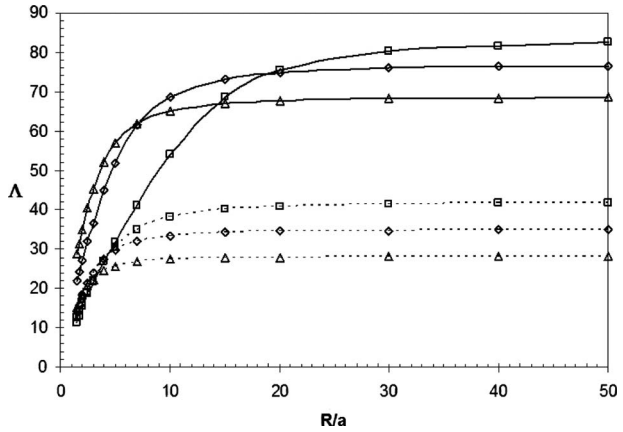

Fig. 2 The first three frequency parameters of symmetric and antisymmetric modes about the coordinate φ for the C-C sectors when the sectors make symmetric vibrations about their centerline plane. Solid line: the symmetric mode; dash line: the antisymmetric mode; □: φ_0=120 deg; ◇:φ_0=180 deg; △: φ_0 =240 deg.

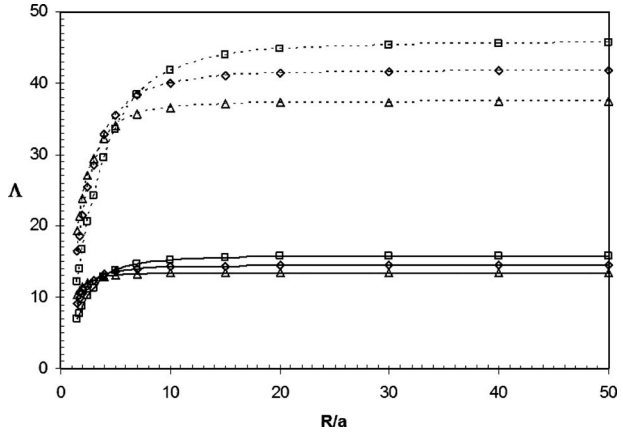

Fig. 3 The first three frequency parameters of symmetric and antisymmetric modes about coordinate φ for the C-C sectors when the sectors make antisymmetric vibrations about their centerline plane. Solid line: the symmetric mode; dash line: the antisymmetric mode; □: φ_0=120 deg; ◇:φ_0=180 deg; △: φ_0 =240 deg.

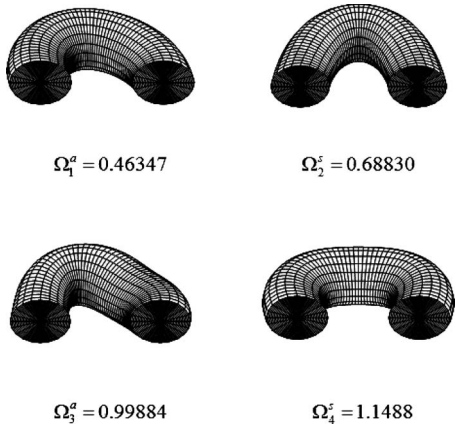

Fig. 4 The first four modes symmetric about the centerline plane for a C-C sector with the subtended angle φ_0=180 deg and the radius ratio R/a=2. The superscript *s* means the symmetric modes in the φ direction and the superscript *a* means the antisymmetric modes in the φ direction.

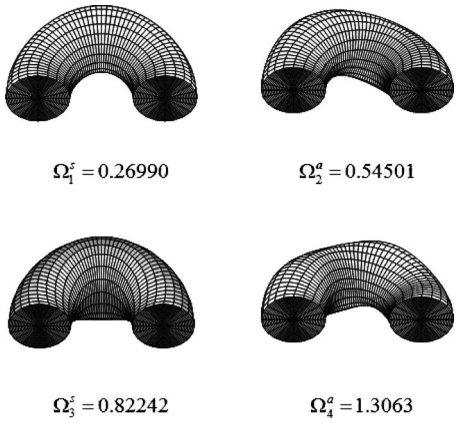

Fig. 5 The first four modes antisymmetric about the centerline plane for a C-C sector with the subtended angle φ_0=180 deg and the radius ratio R/a=2. The superscript *s* means the symmetric modes in the φ direction and the superscript *a* means the antisymmetric modes in the φ direction.

spectrum for curved breams. Through the parametric studies, the variations of eigenfrequency parameters versus the radius ratio and subtended angle of sectors are noted. The results for three-dimensional vibration analysis of circular toroidal sectors with circular cross-section are presented for the first time. Due to the excellent stability of Chebyshev polynomials in numerical computations, the present method allows one to include more terms of admissible functions in the Ritz solution so as to achieve very accurate results whereas other admissible functions such as the simple algebraic polynomials may not be able to do so.

Acknowledgment

The work described in this paper was supported by the CAS membership "structural vibrations in three-dimensional solids" from the University of Hong Kong.

References

[1] Lamb, H., 1887, "On the Flexure and the Vibrations of a Curved Bar," Proc. London Math. Soc., **s1-19**, pp. 365–377.
[2] Love, A. E. H., 1892, "On the Vibrations of an Elastic Circular Ring (Abstract)," Proc. London Math. Soc., **s1-24**, pp. 118–120.
[3] Chidamparam, P., and Leissa, A. W., 1993, "Vibrations of Planar Curved Beams, Rings and Arches," Appl. Mech. Rev., **46**, pp. 467–483.
[4] Eisenberger, M., and Efraim, E., 2001, "In-Plane Vibrations of Shear Deformable Curved Beams," Int. J. Numer. Methods Eng., **52**, pp. 1221–1234.
[5] Montalvão e Silva, J. M. M., and Urgueira, A. P. V., 1988, "Out-of-Plane Dynamic Response of Curved Beams—An Analytical Model," Int. J. Solids Struct., **24**, pp. 271–284.
[6] Irie, T., Yamada, G., and Tanaka, K., 1982, "Natural Frequencies of Out-of-Plane Vibration of Arcs," ASME J. Appl. Mech., **49**, pp. 910–913.
[7] Irie, T., Yamada, G., and Tanaka, K., 1983, "Natural Frequencies of In-Plane Vibrations of Arcs," ASME J. Appl. Mech., **50**, pp. 449–452.
[8] Archer, R. R., 1960, "Small Vibrations of Thin Incomplete Circular Rings," Int. J. Mech. Sci., **1**, pp. 45–56.
[9] Veletsos, A. S., and Austin, W. J., 1972, "Free in-Plane Vibrations of Circular Arches," ASCE J. Eng. Mech., **98**, pp. 311–329.
[10] Austin, W. J., and Veletsos, A. S., 1973, "Free Vibration of Arches Flexible in Shear," ASCE J. Eng. Mech., **99**, pp. 735–753.
[11] Hutchinson, J. R., 1972, "Axisymmetric Vibrations of a Free Finite Length Rod," J. Acoust. Soc. Am., **51**, pp. 233–240.
[12] Hutchinson, J. R., 1980, "Vibrations of Solid Cylinders," ASME J. Appl. Mech., **47**, pp. 901–907.
[13] Leissa, A. W., and Zhang, Z. D., 1983, "On the Three-Dimensional Vibrations of the Cantilevered Rectangular Parallelepiped," J. Acoust. Soc. Am., **73**, pp. 2013–2021.
[14] Lim, C. W., 1999, "Three-Dimensional Vibration Analysis of a Cantilevered Parallelepiped: Exact and Approximate Solutions," J. Acoust. Soc. Am., **106**, pp. 3375–3381.
[15] Hutchinson, J. R., 1981, "Transverse Vibrations of Beams, Exact Versus Approximate Solutions," ASME J. Appl. Mech., **48**, pp. 923–928.
[16] Leissa, A. W., and So, J., 1995, "Comparisons of Vibration Frequencies for Rods and Beams From One-Dimensional and Three-Dimensional Analysis," J. Acoust. Soc. Am., **98**, pp. 2122–2135.

[17] Liew, K. M., Hung, K. C., and Lim, M. K., 1995, "Modeling Three-Dimensional Vibration of Elliptic Bars," J. Acoust. Soc. Am., **98**, pp. 1518–1526.
[18] Liew, K. M., Hung, K. C., and Lim, M. K., 1998, "Vibration of Thick Prismatic Structures With Three-Dimensional Flexibility," ASME J. Appl. Mech., **65**, pp. 619–625.
[19] Zhou, D., Cheung, Y. K., Lo, S. H., and Au, F. T. K., 2003, "3-D Vibration Analysis of Solid And Hollow Circular Cylinders via Chebyshev–Ritz Method," Comput. Methods Appl. Mech. Eng., **192**, pp. 1575–1589.
[20] Zhou, D., Au, F. T. K., Lo, S. H., and Cheung, Y. K., 2002, "Three-Dimensional Vibration Analysis of a Thick Torus With Circular Cross-Section," J. Acoust. Soc. Am., **112**, pp. 2831–2839.
[21] Kang, J. H., and Leissa, A. W., 2006, "Natural Frequencies of Thick, Complete, Circular Rings With an Elliptical or Circular Cross-Section From a Three-Dimensional Theory," Arch. Appl. Mech., **75**, pp. 425–439.
[22] Kang, J. H., and Leissa, A. W., 2000, "Three-Dimensional Vibrations of Thick, Circular Rings With Isosceles Trapezoidal and Triangular Cross-Sections," ASME J. Vibr. Acoust., **122**, pp. 132–139.
[23] Buchanan, G. R., and Liu, Y. J., 2005, "An Analysis of the Free Vibration of Thick-Walled Isotropic Toroidal Shells," Int. J. Mech. Sci., **47**, pp. 277–292.